Journal of Molecular Graphics and Modelling 86 (2019) 35–42

Contents lists available at ScienceDirect

Journal of Molecular Graphics and Modelling

journal homepage: www.elsevier.com/locate/JMGM

Structural analysis of a novel *N*-carbamoyl-D-amino acid amidohydrolase from a Brazilian *Bradyrhizobium japonicum* strain: *In silico* insights by molecular modelling, docking and molecular dynamics

Reinaldo G. Bellini [a], Mônika Aparecida Coronado [b], Alexandre Rossi Paschoal [c], Thaís Gaudencio do Rêgo [d], Mariangela Hungria [e], Ana Tereza Ribeiro de Vasconcelos [a, *], Marisa Fabiana Nicolás [a, **]

[a] Laboratório Nacional de Computação Científica, Petrópolis, Rio de Janeiro, Brazil
[b] Centro Multiusuário de Inovação Biomolecular, Departamento de Física, Universidade, Estadual Paulista (UNESP), São José do Rio Preto, 15054-000, SP, Brazil
[c] Federal University of Technology – Paraná, Avenida Alberto Carazzai, 1640, 86300-000, Cornélio Procópio, PR, Brazil
[d] Universidade Federal da Paraíba, Centro de Informática, Rua dos Escoteiros, S/N, João Pessoa, PB, 58055-000, Brazil
[e] Embrapa Soja, Cx. Postal 231, 86001-970, Londrina, PR, Brazil

ARTICLE INFO

Article history:
Received 17 June 2018
Received in revised form
6 October 2018
Accepted 8 October 2018
Available online 9 October 2018

Keywords:
N-Carbamoyl-D-amino acid amidohydrolase
Docking
Molecular modelling
Molecular dynamics
D-amino acids
Bradyrhizobium japonicum

ABSTRACT

In this work we performed several *in silico* analyses to describe the relevant structural aspects of an enzyme *N*-Carbamoyl-D-amino acid amidohydrolase (D-NCAase) encoded on the genome of the Brazilian strain CPAC 15 (=SEMIA 5079) of *Bradyrhizobium japonicum*, a nonpathogenic species belonging to the order Rhizobiales. D-NCAase has wide applications particularly in the pharmaceutical industry, since it catalyzes the production of D-amino acids such as D-*p*-hydroxyphenylglycine (D-HPG), an intermediate in the synthesis of β-lactam antibiotics. We applied a homology modelling approach and 50 ns of molecular dynamics simulations to predict the structure and the intersubunit interactions of this novel D-NCAase. Also, in order to evaluate the substrate binding site, the model was subjected to 50 ns of molecular dynamics simulations in the presence of *N*-Carbamoyl-d-*p*-hydroxyphenylglycine (Cp-HPG) (a D-NCAase canonical substrate) and water-protein/water-substrate interactions analyses were performed. Overall, the structural analysis and the molecular dynamics simulations suggest that D-NCAase of *B. japonicum* CPAC-15 has a homodimeric structure in solution. Here, we also examined the substrate specificity of the catalytic site of our model and the interactions with water molecules into the active binding site were comprehensively discussed. Also, these simulations showed that the amino acids Lys123, His125, Pro127, Cys172, Asp174 and Arg176 are responsible for recognition of ligand in the active binding site through several chemical associations, such as hydrogen bonds and hydrophobic interactions. Our results show a favourable environment for a reaction of hydrolysis that transforms *N*-Carbamoyl-d-*p*-hydroxyphenylglycine (Cp-HPG) into the active compound D-*p*-hydroxyphenylglycine (D-HPG). This work envisage the use of D-NCAase from the Brazilian *Bradyrhizobium japonicum* strain CPAC-15 (=SEMIA 5079) for the industrial production of D-HPG, an important intermediate for semi-synthesis of β-lactam antibiotics such as penicillins, cephalosporins and amoxicillin.

1. Introduction

N-carbamoyl-D-amino acid amidohydrolase (EC 3.5.1.77) known as D-NCAase or Dcase is an amidohydrolase that catalyzes the production of D-amino acid from *N*-carbamoyl-D-amino acid. This enzyme is selective for *N*-carbamoyl D-amino acids, not acting on

* Corresponding author.
** Corresponding author.
E-mail addresses: monikacoronado@gmail.com (M.A. Coronado), paschoal@utfpr.edu.br (A.R. Paschoal), gaudenciothais@gmail.com (T. Gaudencio do Rêgo), hungria@cnpso.embrapa.br (M. Hungria), atrv@lncc.br (A.T. Ribeiro de Vasconcelos), marisa@lncc.br (M.F. Nicolás).

https://doi.org/10.1016/j.jmgm.2018.10.005

the corresponding L-amino acids or *N*-formyl amino acids [1]. D-amino acids are of great interest to the pharmaceutical and biotechnology industry, since they are intermediaries for the production of synthetic antibiotics, peptide hormones and pesticides. The main industrial process for the production of D-amino acids involves the following steps: i) chemical synthesis of hydantoin, ii) stereospecific hydrolysis of hydantoins catalyzed by microbial enzyme D-hydantoinase (EC 3.5.2.2) and, iii) removal of carbamoyl. The removal of carbamoyl has been performed using the chemical treatment of the intermediaries (*N*-carbamoyl-D-amino acid) with an equimolar amount of nitrite under acidic conditions [2]. However, applying a simpler and less pollutant process, this last chemical method may be replaced by a second enzymatic step using D-NCAase [3,4]. This enzyme can produce D-amino acids from various *N*-carbamoyl-D-amino acids, such as D-*p*-hydroxyphenylglycine (D-HPG), which is an intermediate essential for the synthesis of penicillin, cephalosporin and amoxicillin [5]. Most studies with D-NCAase have been performed with proteins from the genus *Agrobacterium* [3,6–9]. D-NCAases orthologous share medium identity of amino acid sequence, for example, D-NCAase of *Agrobacterium* spp. shows 61% of identity with that of *Pseudomonas* spp [10]. The crystallographic structure of D-NCAase protein has been described in its homotetrameric form in *Agrobacterium* spp. strain KNK712 (PDB code: 1ERZ) and in *A. radiobacter* (currently known as *Rhizobium radiobacter*) (PDB codes: 1FO6, 2GGK and, 2GGL). Site-directed mutagenesis and biochemical analysis suggest that the residue Cys172 is a target for sulfhydryl reagents and it has been proposed as the probable residue of the active site [3]. Although the crystallographic structure of D-NCAase was initially described as being homotetrameric, studies carried out by Grifantini et al. (1996) and Wang et al. (2001) with the enzymes isolated from *A. radiobacter* indicate that this enzyme exists as a homodimer in solution, consisting of two identical subunits of 34 kDa [3,9]. Similarly, a D-NCAase purified from *Pseudomonas* sp. strain KNK003A seems to be a homodimer with MW of approximately 38 kDa and specific activity for *N*-carbamoyl-D-amino acids [10]. In contrast, the enzymes of *Blastobacter* spp. and *Comamonas* spp. were identified as a homotrimer, with MW of approximately 40 kDa [4,11]. These studies indicate that the biologically active form of the D-NCAase from different sources is organized in more than one subunit. Consequently, the structural biodiversity can be exploited in order to evaluate and optimize the catalytic activity and stability of the orthologous enzymes. Noteworthy, is that most studies with D-NCAase have been performed with proteins from *A. Radiobacter* [3,6–9], an opportunistic pathogen in human. For this reason, since the late 1980's scientists seek for the identification of D-NCAases in nonpathogenic bacteria. Consequently, orthologous D-NCAase enzymes were identified in *Blastobacter* spp. [11], *Comamonas* spp. [4], *Pseudomonas* sp. strain KNK003A [10] and *Ensifer adhaerens* (old *Sinorhizobium morelens*) strain S-5 [12]. Here, we describe for the first time an orthologous D-NCAase from the species *Bradyrhizobium japonicum,* namely Brazilian *B. japonicum* strain CPAC-15 (=SEMIA 5079), a nonpathogenic bacteria belonging to the order Rhizobiales and broadly used in commercial inoculants for the soybean crop in Brazil [13]. Thus, we present a model and discuss the new orthologous enzyme, which should contribute towards understanding this enzyme that catalyzes the production of D-amino acids required for semi-synthesis of β-lactam antibiotics.

2. Methods

2.1. Sequence data and primary analysis

The atomic coordinates of *N*-carbamoyl-D-amino-acid amidohydrolase from *Agrobacterium radiobacter* CCRC 14924 (PDB code: 1FO6) solved at 1.95 Å resolution was used as a template [9]. Homology modelling was performed by SWISS-MODEL approach [14]. Geometric parameters including Ramachandran plots, bonds and angle deviations were evaluated using the web server RAMPAGE [15].

2.2. Molecular dynamics (MD) simulations of D-NCAase of B. japonicum strain CPAC-15

After homology modelling, two models were simulated by molecular dynamics, namely the homotetramer (Four chains A, B, C and D) and the homodimer (chains A and B). The molecular dynamics were performed for relaxing structure using Gromacs simulation package [16] using a rectangular box with 10 Å distance from the protein at each direction. The OPLS-AA force field [16,17] was used to describe the all atoms and for water model the TIP4P was used [18,19]. Newton's equations of motion were integrated using the leapfrog scheme with a time step of 2 fs All bond lengths were constrained using the LINCS [20] procedure. The electrostatics calculations were evaluated using Particle Mesh Edwald (PME) [20,21]. All systems were neutralized by adding Na^+ and Cl^- counterions. As previously described [22], we chose an optimization approach, which started with the initial homotetramer structure with 100,000 steps of steepest descent algorithm that was used following 100,000 steps of conjugated gradient to optimize the protein structure. Following, the system was equilibrated for 10 ns in a NPT (constant numbers of particles N, pressure P, and temperature T) with 298 K of temperature and pressure of 1 Bar. The algorithms in this phase for temperature and pressure coupling were v-rescale and Berendsen, respectively. For the production phase of molecular dynamics, both the homotetrameric and homodimeric molecules were simulated during 50 ns with NPT ensemble. In addition, for this phase, the Nose-Hoover and Parrinello-Rahman dynamics/methods were used to maintain the temperature and pressure constant. At the end of the molecular dynamics, radius of gyration and RMSD were measured to verify the equilibration of the system. Also, the binding free energy calculation was performed from the snapshots of MD trajectory (last 10 ns) using the molecular mechanics Poisson-Boltzmann surface area (MM/PBSA) method by the g_mmpbsa tool of GROMACS (https://rashmikumari.github.io/g_mmpbsa) [16].

2.3. Ligand optimization and docking protocol

The *N*-Carbamoyl-d-*p*-hydroxyphenylglycine (Cp-HPG), which is a common substrate used in D-NCAase enzyme assays [4] was docked to the modelled structure of D-NCAase of *B. japonicum* CPAC-15. The ligand was first optimized with a DFT functional theory, with a 3.21 G basis by Gaussian 08 [23]. The atomic charges obtained in this procedure along with the topological information of the ligand (rotatable bonds) were used for molecular dynamics calculations. For docking, we use the DockThor algorithm [24], a flexible receptor ligand docking. The grid box was centered on the alpha carbon of Cys172 that is localized at the bottom of the active site pocket. The search space was a rectangular box covering the entire surface and centered on the geometric center of the Cys172 extending 10 Å beyond the residue edge in each direction. In this procedure, a genetic algorithm was used with 1,000,000 evaluations and a population of 1000 individuals with 30 runs. The score function used was MMFF94 [25]. To perform a virtual screening experiment and search of compounds were used Zinc database (http://zinc.docking.org) and IVIEW web server (http://istar.cse.cuhk.edu.

hk/idock), respectively.

3. Results and discussion

3.1. Primary sequence analysis

By searching for an orthologous enzyme of D-NCAase in the genome of *B. japonicum* strain CPAC-15 we found a sequence of 310 aa (GenBank: AHY51785.1/SEMIA 5079) (Supplementary material Figure S1). The identity of the deduced amino acid sequence of this enzyme with that of *Agrobacterium radiobacter* CCRC 14924 (PDB: 1FO6) was 51.84%. Fig. 1 shows a multiple sequence alignment among D-NCAase enzymes of *B. japonicum*, *A. radiobacter*, *Pseudomonas* sp and *E. Adhaerens*, which denotes high conservation of amino acid residues and that the amino acid sequence of CPAC-15 enzyme is longer than the other ones. The conserved cysteine residues are highlighted in the multiple alignment as well as the amino acids highly conserved related to the active site pocket (Glu47, Lys123, Glu142 and Cys172) (Fig. 1).

3.2. Protein structure homology modelling: assessing the intersubunit interactions

In this study, the D-NCAase models of *B. japonicum* CPAC-15 were generated through homology modelling using the SWISS-MODEL server [14]. Two SWISS-MODEL parameters used were: (i) the GMQE (Global Model Quality Estimation) objective function, which is an estimate of the quality between the template alignment and the generated model. The result is a score that returns a normalized value in the interval 0 to 1 reflecting the accuracy of the model; (ii) the crystal resolution when obtained by X-ray crystalography.

In this work the two best structures obtained were PDB codes: 1FO6 and 1UF5 with GMQE 0.76 and 0.77, respectively. The choice for the PDB: 1FO6 structure as a template was due to its high crystallographic resolution (2.0 Å).

Initially, a homotetrameric structure was obtained by homology modelling, composed of chains A, B, C, and D (Fig. 2a). The quality of the predicted structure was confirmed evaluating the stereochemical properties of this model. Fig. 2b depicts the modelled D-

Fig. 1. Multiple sequence alignment (by CLUSTALW [29]) among D-NCAase of *B. japonicum* CPAC-15, *Agrobacterium radiobacter* strains CCRC 14924 and NRRL-B11291 (RHID-1FO6), *Pseudomonas* sp strain KNK003A (PSED-KNK003A) and *Ensifer adhaerens* (ENSAD-S-S). The red box shows the conserved cysteine residues. The arrow shows the catalytic triad responsible for the activity of the enzyme.

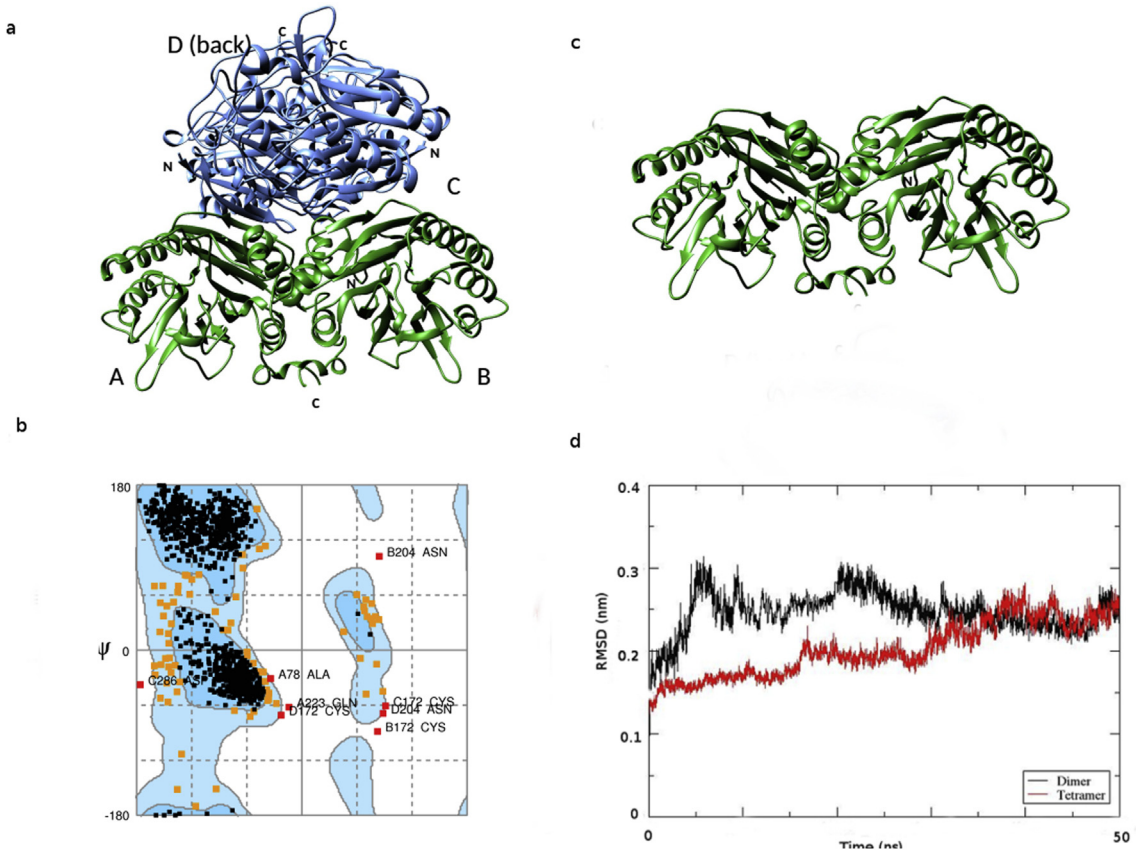

Fig. 2. Schematic diagrams. a) Cartoon representation of the homotetrameric structure of D-NCAase CPAC-15. b) Ramachandran plot of homotetrameric form of D-NCAase of *B. japonicum* CPAC-15 obtained by homology modelling. c) Cartoon representation of the homodimeric structure of D-NCAase CPAC-15. d) Enzyme backbone root mean square deviations (RMSD) during 50 ns of MD showing the trajectories of both, homodimeric (black curve) and homotetrameric (red curve) forms of D-NCAase CPAC-15. Note that equilibrium phase is reached after 30 ns.

NCAase in a homotetrameric form represented in the corresponding Ramachandran Plot, by which it can be deduced that 95% of the residues are in the favourable regions and 2% in the allowed one. This result indicates that all phi-psi angles of amino acids of the modelled D-NCAase are in correct orientation to form the fold of this enzyme.

To estimate the stability of the modelled D-NCAase of *B. japonicum* CPAC-15, the enzyme backbone root mean square deviations (RMSD) was monitored throughout the 50 ns MD simulation for both, the homotetrameric and homodimeric forms. Both systems reached convergence and stabilization after 30 ns (Fig. 2d). RMSD deviation of the modelled D-NCAase of *B. japonicum* CPAC-15 after 50 ns was <1.009 Å with the template PDB: 1FO6.

In the modelled homotetrameric structure the intersubunit contacts among the four chains are very different (Fig. 2a). Subunits A and B form a tight dimer, whereas the interaction of the A-D subunits and of the A-C subunits is looser, which may suggest a stable AB dimer for this D-NCAase. Also, since the orthologous enzyme identified in the Rhizobiaceae family member, *A. Radiobacter* [3] has been shown to form a homodimer in aqueous solution, we investigated the same conformation in the orthologous enzyme of *B. japonicum* CPAC-15. Thus, in order to investigate whether D-NCAase of *B. japonicum* strain CPAC-15 can form a homodimeric structure in solution we performed 50 ns of MD simulation. When we analyzed the architecture of the homotetrameric form after 50 ns of MD, the homodimeric subunits were packed tightly against each other with about 90° of rotation (Fig. 2a). These rotations suggest asymmetric interactions among different homodimeric subunits of this modelled enzyme. To verify a homodimeric formation we performed an analysis of interactions between chains A-B, A-C and A-D using the Protein Interactions Calculator (PIC) algorithm [26]. The PIC algorithm recognizes various types of interactions; such as disulphide bonds, hydrophobic interactions, ionic interactions, hydrogen bonds, aromatic-aromatic interactions, aromatic-sulphur interactions and cation-π interactions within a protein or between proteins in a complex. The results showed that for A and B subunits there are 38 hydrogen bonds, whereas for A and D subunits there are only 20 hydrogen bonds and no hydrogen bond was found for the A and C subunits. When we considered the hydrophobic contacts, we found 31 interactions for A and D subunits, while just one contact for A and C subunits and no interactions for A and D subunits was found. The higher number of both hydrogen bond and hydrophobic contacts of interface between only two subunits suggest a homodimeric formation in solution for the D-NCAase of *B. japonicum* strain CPAC-15. This homodimeric organization was also shown for the D-NCAase of *A. radiobacter* through SDS-PAGE analyses performed by Griffantini et al. (1996) [3]. In addition, the authors point out that, although the enzyme contains five cysteine residues, the enzyme was found to be organized in a non-disulfide bonded homodimeric structure. Thus, we also investigated the role of cysteine residues for the disulfide bond in the modelled D-NCAase of CPAC-15, as well as the active site pocket as discussed in the next section.

3.3. Cysteine residues and the active site pocket

It is well known that disulfide bonds are responsible for stabilizing folding and covalent assembly and this process is associated with thiol groups in cysteine residues. In light of this evidence, we investigated the cysteine residues inside the structure of homodimeric D-NCAase of *B. japonicum* CPAC 15. Accordingly, there are five cysteine residues per protein chain, *i.e.* Cys107, Cys172, Cys193, Cys252 and Cys281 (Fig. 1). Fig. 3 shows the position of these five cysteine residues inside this enzyme structure. Cys193 and Cys252, both were localized in a beta-sheet and Cys281 close to the external loop and outside of the protein core. Cys107 is localized in a beta-sheet and Cys172 lies at the bottom of the active site pocket, as reported previously [3]. Also, an analysis of the prediction of cysteine residues solvent accessibility after 50 ns of MD confirmed that Cys172 is the only amino acid residue accessible to the solvent (see also next section 3.4), which is in line with previous results [3]. As mentioned before, Grifantini et al. (1996) studied the role of the five cysteine residues in the biological activity of the D-NCAase of *A. radiobacter* NRRL B11291 using chemical and genetic methods. These authors demonstrated that the five cysteine residues Cys172, Cys193, Cys243, Cys250 and Cys279 (Fig. 1) present in the enzyme are not engaged in intramolecular disulfide bonds [3]. In view of four cysteine residues present in the D-NCAase of *A. radiobacter* NRRL B11291 are conserved in the CPAC-15 enzyme (Fig. 1) we performed 50 ns of MD analysis and measured the distances among all cysteine pairs. This analysis showed that in the D-NCAase of *B. japonicum* CPAC-15 the five cysteine residues are not involved in intramolecular disulfide bonds.

To estimate the number of water molecules within the active site pocket, we monitored the hydrogen bonds between Cys172 and water molecules during the final 10 ns of the 50 ns of MD. The average number of hydrogen bonds during the equilibrium of system was 5.26 ± 0.66 (angle 30° and distance considered of 3.5 Å). This result indicates that for each time step of MD, the Cys172 formed five hydrogen bonds, approximately. After 50 ns of MD simulations we observed an average of 4.53 ± 1.24 water molecules interacting with Cys172 inside the binding site. Fig. 4 shows the snapshot of four water molecules that interact with Cys172 at distance of 3.5 Å. Similar results were observed by Wang et al. (2001) in a homodimeric D-NCAase of *A. radiobacter* estimating eight water molecules interacting with Cys172 [9]. These results suggest a favourable environment for the hydrolysis reaction, a crucial requirement within the active site pocket for transforming a D-NCAase substrate such as Cp-HPG to the optically active compound D-HPG (discussed at section 3.4).

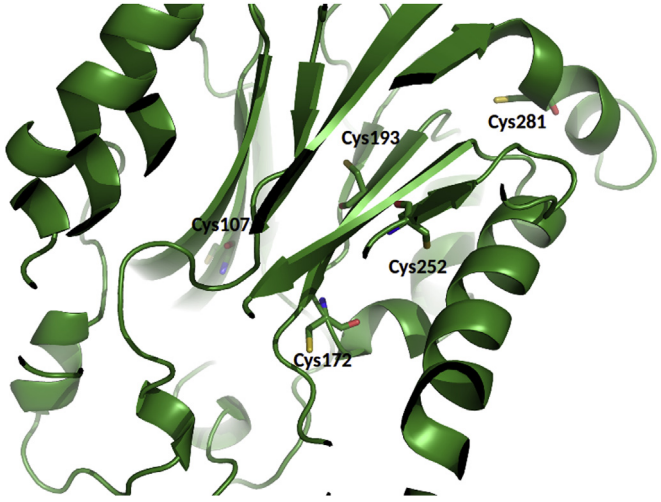

Fig. 3. Cartoon representation of D-NCAase CPAC-15 model. Highlighted in stick are the five cysteine residues presented in our model. Figure was generated by PyMol (www.pymol.org).

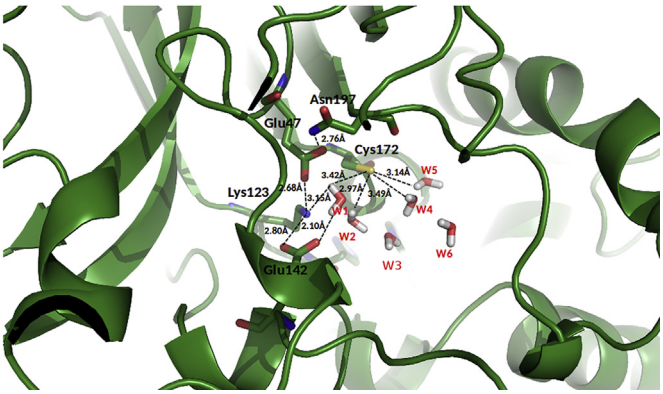

Fig. 4. Cartoon representation of the active site pocket. Hydrogen bonds of the catalytic residue Cys172 with water molecules are shown and other mino acids at the bottom of the active site pocket are highlighted.

Regarding the active site pocket in the template PDB: 1FO6, the conserved amino acids His129, His144 and His215 are responsible for its conformation [9]. In this work, the modelled D-NCAase of *B. japonicum* CPAC-15 maintains both His129 and His215 as conserved residues of the active site pocket, whereas the His144 is replaced by Gln140 (see alignment Fig. 1). As shown above, the substitution of the amino acid H140Q in the CPAC-15 enzyme would not interfere with the conformation of the active site pocket of the modelled D-NCAase of *B. japonicum* CPAC-15.

Considering the chain A, there are six water molecules inside the active site pocket (Fig. 4) surrounded by 19 amino acids (Glu47, Phe53, Lys123, His125, Leu126, Pro127, Gln140, Glu142, Ile171, Cys172, Asp174, Arg176, Tyr196, Asn197, Ser198, Ala199, Arg296, Glu298, Gln299, data not shown). Eleven of these amino acids are conserved between the D-NCAase of *B. japonicum* CPAC-15 and the template PDB: 1FO6 (Glu47, Phe53, Lys123, Leu126, Pro127, Glu142, Ile171, Cys172, Asp174, Tyr196 and Asn197, Fig. 1), four of them being highly conserved (Glu47, Lys123, Glu142, Cys172 among *Agrobacterium*, *Pseudomonas,* and *Methanobacter* [9]. The stabilization of Lys123 is formed by hydrogen bonds with residues Glu47 and Glu142, and a water molecule. The Glu47 and Glu142 are stabilized through interaction with Asn197 and a water molecule, respectively (Fig. 4). On the other hand, we observed that the first solvation shell around the Cys172 at distances less than 3.5 Å consists of 6 ± 1.41 water molecules forming 5.26 ± 0.66 hydrogen bonds during the final 10 ns of MD simulations.

3.4. Ligand-protein interactions

The substrate specificity of D-NCAase for *N*-carbamoyl-D-amino acids has already been reported. These lines of evidence indicated that the active site of D-NCAase recognizes only the *N*-carbamoyl and α-carboxyl group of a *N*-carbamoyl-D-amino acid, which depends on the steric hindrance. That implies that the fixed orientation of these moieties allows a relatively large volume for a side-chain of D-enantiomer, instead there is very limited space for a side-chain of the L-enantiomer [7,9,27]. In this study to verify the specificity of the catalytic site of our model, we evaluated the ligand affinity toward active site of D-NCAase of *B. japonicum* CPAC-15 against more than 100 compounds. For that, initially we performed a virtual screening experiment, recovered and analyzed the

result of 100 compounds from the Zinc database (http://zinc.docking.org). The search for compounds was conducted using the Cp-HPG as a query through the IVIEW web server (http://istar.cse.cuhk.edu.hk/idock), which compares both the 3D shape of two molecules and the spatial distribution of atom types relevant for molecular recognition (aromatic, hydrogen bond donor, hydrogen bond acceptor and hydrophobic atoms). The first 100 more similar molecules to the query out of the 23 million screened were returned. After this procedure, the 100 compounds as well as the canonical D-NCAase substrate (Cp-HPG) and its L-enantiomer were docked with the enzyme using DockThor algorithm [24]. Table S1 shows the potential energy for the docking between this D-NCAase and each ligand. The interactions were evaluated through the interaction energy. As shown in Table S1, the list of 102 compounds docked with D-NCAase CPAC-15 highlights the Cp-HPG as the compound with the best interaction in terms of the potential energy (−39.453 kcal/mol), which indicates a highest affinity of D-NCAase for Cp-HPG.

Despite the interactions with other compounds seem to be favourable, the resulting products would not generate D-amino acid derivatives. This is also the case of the complex with the L-enantiomer of Cp-HPG. Particularly, when we anchored the L-enantiomer with the D-NCAase CPAC-15, we observed that the interaction distance between L-enantiomer and both residues Cys172 and Arg176 was larger than with the D-enantiomer, so no hydrogen bond is formed as observed with D-enantiomer. In addition, due to a conformational change of L-enantiomer, the His125 (that interacts with the ring of the D-enantiomer but is not part of the catalytic triad) interacts with the α-carboxyl group of the L-enantiomer suggesting the observed favourable energy of interaction (−36,620 kcal/mol). These results are in agreement with the previous reports [7,9,27].

As shown by Wen-Ching Wang et al. (2001) [9], the catalytic reaction for D-NCAse with D-enantiomer mediated by the amino acids Cys172, Glu47 and Lys123 occurs through the nucleophilic attack of Cys172 (S) to (C) of the carbamoyl group of the ligand. We observed that this reaction is unfavourable with L-enantiomer, because in comparison with D-enantiomer there is an increase in the interaction distance between Cys172 (S) and C of the carmaboyl group in 89%, which prevents the nucleophilic attack. Thus, the remaining stages of the cascade reaction would not occur, then avoiding the catalysis. Finally, binding at the active site by the L-enantiomer can occur, but the catalytic reaction does not, so this L-enantiomer can act as an antagonist compound.

To further understand the role of the amino acids involved in the catalysis and the substrate binding, first we carried out docking using the ligand Cp-HPG, and then we run 50 ns of MD simulations with the ligand-enzyme complex. Fig. 5 shows the snapshot from the MD trajectory with the interactions responsible for stabilizing the ligand Cp-HPG into the active site of D-NCAase of *B. japonicum*. From Fig. 5 it can be noticed that Lys123, His125, Pro127, Cys172, Asp174 and Arg176 are the amino acids responsible for keeping the ligand Cp-HPG into the active site. The α-carboxyl group of the ligand Cp-HPG interacts directly with Cys172, with a distance of 3.3 Å, which is in agreement with previous results shown by Wang et al. (2001) [9]. Also, as mentioned before, water molecules were located near the ligand binding site, which can contribute to the hydrolysis reaction (Fig. 5).

We have also determined the important interactions between water molecules, ligand and amino acids within the cavity of the active site as shown in Fig. 5. The hydrogen bonds between the ligand Cp-HPG and water molecules in the equilibrium after 50 ns of MD simulations had an average number of 5.65 ± 1.30 considering a distance cutoff/threshold of 3.5 Å. Interactions between water molecules and amino acids and water molecules and

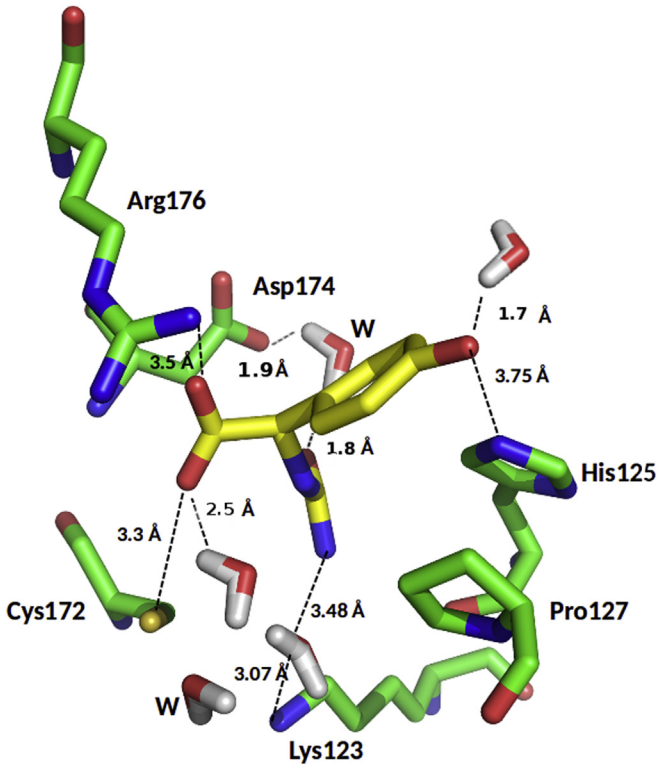

Fig. 5. The amino acids of the active site pocket in the D-NCAase model (green) with Cp-HPG ligand (yellow) are shown. Figure was generated by PyMol (www.pymol.org). (For interpretation of the references to colour in this figure legend, the reader is referred to the Web version of this article.)

substrate are relevant interaction for maintaining the stability of a ligand within the binding site. We verified two of these interactions between Lys123-water and water-Cp-HPG at 3.07 Å and 3.48 Å, with an average of 3.07 ± 0.26 and 3.18 ± 0.22 respectively, as well as between Asp174-water and water-Cp-HPG at 1.9 Å and 1.84 Å, with an average of 2.66 ± 0.50 and 2.74 ± 0.5, respectively. Thus, these interactions can contribute to the hydrolysis reaction meditated by the CPAC-15 enzyme (Fig. 5).

Regarding the charge related to the amino acid associated with the active site of the enzyme (Fig. 1), we noted that 50% are positively charged, 33.33% have hydrophobic characteristics and 16.6% are negatively charged. Interesting D-NCAase possesses preference for substrates which have a long/bulky hydrophobic side-chain. This suggests that a substrate providing more van der Waals contacts can bind better in this pocket that is predominantly hydrophobic and positively charged [Wen-Ching Wang et al. (2001)]. Indeed, the large volume enclosing the hydroxyphenyl group of the Cp-HPG is favourable for more van der Waals contacts [28].

Here, we examined the interaction energies (including the van der Waals and electrostatic) of the substrate in the complex D-NCAase-Cp-HPG. We found that the average van der Waals and electrostatic energies are −82.49 kJ/mol and −24.15 kJ/mol, respectively. These results indicate that the complex is maintained mainly for van der Waals interactions according with previous results.

Thus, in terms of structure of a ligand regarding the development of a D-NCAase modulators, it should be noted a long/bulky hydrophobic side-chain of a substrate that would be providing an enhanced binding.

Further to determine the contribution of each residue to the total binding energy in the interaction D-NCAase-Cp-HPG, we performed a free energy decomposition analysis and calculated the

biding energy per residue. Through this analysis we noted that the residues with major contribution are Asp174 (−4.65 ± 1.26 kJ/mol), Cys172 (−4.21 ± 2.65, kJ/mol), Arg176 (−2.94 ± 2.38 kJ/mol), His125 (−1.18 ± 0.96 kJ/mol, Lys123 (−0.36 ± 0.22 kJ/mol), Pro127 (−0.23 ± 0.15 kJ/mol) and Glu47 (−0.008 ± 0.02 kJ/mol). If the focus were to work on the molecular design of a modulator, the residues to use as anchor should be mainly Asp174, Cys172, Arg176 for α-carboxyl group, His125 for hydroxyl group and Lys123, Pro127, Glu47, Cys172 for *N*-carbamoyl group.

3.5. Data repository

Structural models described in this study are available on the Mendeley Data Repository [30].

4. Conclusions

The enzymes belonging to amidohydrolase superfamily catalyze the hydrolysis of a wide range of substrates. The *N*-carbamoyl-D-amino acid amidohydrolase is used in the industry for the production of D-amino acids. Here, using several *in silico* approaches, for the first time we describe a theoretical structure of *N*-carbamoyl-D-amino acid amidohydrolase of *B. japonicum* strain CPAC-15 (=SEMIA 5079), a nonpathogenic bacterium broadly used in Brazil as an inoculant for soybean crops. Our results suggest a homodimeric structure for this enzyme. By molecular docking and molecular dynamic studies using the enzyme substrate complex, we have shown that this novel D-NCAase may have specific activity for biosynthesis of D-amino acids, such as D-HPG, an important intermediate for semi-synthesis of β-lactam antibiotics. Additionally, we have presented a theoretical investigation on substrate specificity and the interactions with water molecules into the active binding site were comprehensively discussed. Finally, we examined the contribution of each residue to the total binding energy in the interaction D-NCAase-Cp-HPG getting insight into the design of other kinds of modulators for this target protein.

Declarations of interest

None.

Funding

This work was supported by the Coordenação de Aperfeiçoamento de Pessoal de Nível Superior (process no. 23038.010041/2013–13) and the Conselho Nacional de Desenvolvimento Científico e Tecnológico (process no. 307713/2016–4) through grants awarded to ATRV and MFN, respectively.

Appendix A. Supplementary data

Supplementary data to this article can be found online at https://doi.org/10.1016/j.jmgm.2018.10.005.

References

[1] S. Martínez-Rodríguez, F.J. Las Heras-Vázquez, L. Mingorance-Cazorla, J.M. Clemente-Jiménez, F. Rodríguez-Vico, Molecular cloning, purification, and biochemical characterization of hydantoin racemase from the legume symbiont Sinorhizobium meliloti CECT 4114, Appl. Environ. Microbiol. 70 (2004) 625–630.
[2] D. Zhang, F. Zhu, W. Fan, R. Tao, H. Yu, Y. Yang, W. Jiang, S. Yang, Gradually accumulating beneficial mutations to improve the thermostability of N-carbamoyl-D-amino acid amidohydrolase by step-wise evolution, Appl. Microbiol. Biotechnol. 90 (2011) 1361–1371.
[3] R. Grifantini, C. Pratesi, G. Galli, G. Grandi, Topological mapping of the cysteine residues of N-carbamyl-D-amino-acid amidohydrolase and their role in enzymatic activity, J. Biol. Chem. 271 (1996) 9326–9331.
[4] J. Ogawa, S. Shimizu, H. Yamada, N-carbamoyl-D-amino acid amidohydrolase from Comamonas sp. E222c purification and characterization, Eur. J. Biochem. 212 (1993) 685–691.
[5] X. Hu, B. Lin, Efficient production of D-HPG with an immobilized transgenic strain E. coli LY13-05, Biotechnol. Biotechnol. Equip. 29 (2015) 1003–1010.
[6] W.H. Hsu, F.T. Chien, C.L. Hsu, T.C. Wang, H.S. Yuan, W.C. Wang, Expression, crystallization and preliminary X-ray diffraction studies of N-carbamyl-D-amino-acid amidohydrolase from Agrobacterium radiobacter, Acta Crystallogr. D Biol. Crystallogr. 55 (1999) 694–695.
[7] T. Nakai, T. Hasegawa, E. Yamashita, M. Yamamoto, T. Kumasaka, T. Ueki, H. Nanba, Y. Ikenaka, S. Takahashi, M. Sato, T. Tsukihara, Crystal structure of N-carbamyl-D-amino acid amidohydrolase with a novel catalytic framework common to amidohydrolases, Structure 8 (2000) 729–737.
[8] H. Nanba, Y. Ikenaka, Y. Yamada, K. Yajima, M. Takano, S. Takahashi, Isolation of Agrobacterium sp. strain KNK712 that produces N-carbamyl-D-amino acid amidohydrolase, cloning of the gene for this enzyme, and properties of the enzyme, Biosci. Biotechnol. Biochem. 62 (1998) 875–881.
[9] W.C. Wang, W.H. Hsu, F.T. Chien, C.Y. Chen, Crystal structure and site-directed mutagenesis studies of N-carbamoyl-D-amino-acid amidohydrolase from Agrobacterium radiobacter reveals a homotetramer and insight into a catalytic cleft, J. Mol. Biol. 306 (2001) 251–261.
[10] J. Ogawa, S. Shimizu, Beta-ureidopropionase with N-carbamoyl-alpha-L-amino acid amidohydrolase activity from an aerobic bacterium, Pseudomonas putida IFO 12996, Eur. J. Biochem. 223 (1994) 625–630.
[11] J. Ogawa, M.C. Chung, S. Hida, H. Yamada, S. Shimizu, Thermostable N-carbamoyl-D-amino acid amidohydrolase: screening, purification and characterization, J. Biotechnol. 38 (1994) 11–19.
[12] S. Wu, Y. Liu, G. Zhao, J. Wang, W. Sun, Thermostable D-carbamoylase from Sinorhizobium morelens S-5: purification, characterization and gene expression in Escherichia coli, Biochimie 88 (2006) 237–244.
[13] A.F. Siqueira, E. Ormeño-Orrillo, R.C. Souza, E.P. Rodrigues, L.G.P. Almeida, F.G. Barcellos, J.S.S. Batista, A.S. Nakatani, E. Martínez-Romero, A.T.R. Vasconcelos, M. Hungria, Comparative genomics of Bradyrhizobium japonicum CPAC 15 and Bradyrhizobium diazoefficiens CPAC 7: elite model strains for understanding symbiotic performance with soybean, BMC Genomics 15 (2014) 420.
[14] T. Schwede, J. Kopp, N. Guex, M.C. Peitsch, SWISS-MODEL: an automated protein homology-modeling server, Nucleic Acids Res. 31 (2003) 3381–3385.
[15] S.C. Lovell, I.W. Davis, W. Bryan Arendall, P.I.W. de Bakker, J. Michael Word, M.G. Prisant, J.S. Richardson, D.C. Richardson, Structure validation by Cα geometry: ϕ,ψ and Cβ deviation, Proteins: Struct. Funct. Bioinf. 50 (2003) 437–450.
[16] S. Pronk, S. Páll, R. Schulz, P. Larsson, P. Bjelkmar, R. Apostolov, M.R. Shirts, J.C. Smith, P.M. Kasson, D. van der Spoel, B. Hess, E. Lindahl, GROMACS 4.5: a high-throughput and highly parallel open source molecular simulation toolkit, Bioinformatics 29 (2013) 845–854.
[17] M.J. Robertson, J. Tirado-Rives, W.L. Jorgensen, Improved peptide and protein torsional energetics with the OPLSAA force field, J. Chem. Theor. Comput. 11 (2015) 3499–3509.
[18] J.L.F. Abascal, C. Vega, A general purpose model for the condensed phases of water: TIP4P/2005, J. Chem. Phys. 123 (2005) 234505.
[19] A.V. Onufriev, S. Izadi, Water models for biomolecular simulations, Wiley Interdiscip. Rev. Comput. Mol. Sci. 8 (2017) e1347.
[20] B. Hess, H. Bekker, H.J.C. Berendsen, G.E. Johannes, LINCS: a linear constraint solver for molecular simulations, J. Comput. Chem. 18 (1997) 1463–1472.
[21] U. Essmann, L. Perera, M.L. Berkowitz, T. Darden, H. Lee, L.G. Pedersen, A smooth particle mesh Ewald method, J. Chem. Phys. 103 (1995) 8577–8593.
[22] R.G. Bellini, A.P. Guimarães, M.A.C. Pacheco, D.M. Dias, V.R. Furtado, R.B. de Alencastro, B.A.C. Horta, Association of the anti-tuberculosis drug rifampicin with a PAMAM dendrimer, J. Mol. Graph. Model. 60 (2015) 34–42.
[23] J. Antony, M.J. Frisch, A.P. Rendell, Modelling the performance of the Gaussian chemistry code on x86 architectures, in: Modeling, Simulation and Optimization of Complex Processes, 2008, pp. 49–58.
[24] C.S. de Magalhães, H.J.C. Barbosa, L.E. Dardenne, Selection-insertion schemes in genetic algorithms for the flexible ligand docking problem, in: Genetic and Evolutionary Computation – GECCO 2004. Lect. Notes Comput. Sci., vol. 3102, 2004, pp. 368–379.
[25] T.A. Halgren, Merck molecular force field. I. Basis, form, scope, parameterization, and performance of MMFF94, J. Comput. Chem. 17 (1996) 490–519.
[26] K.G. Tina, R. Bhadra, N. Srinivasan, PIC: protein interactions calculator, Nucleic Acids Res. 35 (2007) W473–W476.
[27] W.W. Han, D.L. Zhan, Q. L, Y.H. Zhou, Y. Yao, Z.S. Li, Y. Feng, The substrate specificity and the catalytic mechanism of N-carbamyl- D -amino acid amidohydrolase: a theoretical investigation, Chem. Phys. Lett. 472 (2009) 107–112.

[28] C.Y. Chen, W.C. Chiu, J.S. Liu, W.H. Hsu, W.C. Wang, Structural basis for catalysis and substrate specificity of Agrobacterium radiobacter N-carbamoyl- D -amino acid amidohydrolase, J. Biol. Chem. 278 (2003) 26194–26201.

[29] J.D. Thompson, D.G. Higgins, T.J. Gibson, W. CLUSTAL, Improving the sensitivity of progressive multiple sequence alignment through sequence weighting, position-specific gap penalties and weight matrix choice, Nucleic Acids Res. 22 (1994) 4673–4680.

[30] Reinaldo Bellini, Monika Coronado, Alexandre Paschoal, Marisa Nicolás, Ana Vasconselos, Dataset for: Structural analysis of a novel N-carbamoyl-D-amino acid amidohydrolase from a Brazilian Bradyrhizobium japonicum strain: in silico insights by molecular modelling, docking and molecular dynamics, Mendeley Data (2018) v1, https://data.mendeley.com/datasets/vctnmwycht/1.